8-17-2016

Calcification of the Planktonic Foraminiferaglobigerinabulloidesand Carbonate Ion Concentration Resultsfrom the Santa Barbara Basin

Emily B. Osborne

Robert C. Thunell

Brittney J. Marshall

Jessica A. Holm

Eric J. Tappa

See next page for additional authors

Publication Info

Published in *Paleoceanography and Paleoclimatology*, Volume 31, Issue 8, 2016, pages 1083-1102.

AGU PUBLICATIONS

Paleoceanography

RESEARCH ARTICLE
10.1002/2016PA002933

Key Points:
- *G. bulloides* calcification intensity is primarily controlled by ambient seawater [CO_3^{2-}], while size is related to calcification temperature
- The relationship between calcification intensity and [CO_3^{2-}] can be used for past reconstructions of [CO_3^{2-}]
- Morphospecies of G. bulloides found in the Southern California Bight can be identified using shell area density

Supporting Information:
- Supporting Information S1
- Data Set S1
- Data Set S2

Correspondence to:
E. B. Osborne,
eosborne@geol.sc.edu

Citation:
Osborne, E. B., R. C. Thunell, B. J. Marshall, J. A. Holm, E. J. Tappa, C. Benitez-Nelson, W.-J. Cai, and B. Chen (2016), Calcification of the planktonic foraminifera *Globigerina bulloides* and carbonate ion concentration: Results from the Santa Barbara Basin, *Paleoceanography*, *31*, 1083–1102, doi:10.1002/2016PA002933.

Received 9 FEB 2016
Accepted 26 JUL 2016
Accepted article online 30 JUL 2016
Published online 17 AUG 2016

Calcification of the planktonic foraminifera *Globigerina bulloides* and carbonate ion concentration: Results from the Santa Barbara Basin

Emily B. Osborne[1], Robert C. Thunell[1], Brittney J. Marshall[1], Jessica A. Holm[1], Eric J. Tappa[1], Claudia Benitez-Nelson[1], Wei-Jun Cai[2], and Baoshan Chen[2]

[1]School of the Earth, Ocean, and Environment, University of South Carolina, Columbia, South Carolina, USA, [2]College of Earth, Ocean, and Environment, University of Delaware, Newark, Delaware, USA

Abstract Planktonic foraminiferal calcification intensity, reflected by shell wall thickness, has been hypothesized to covary with the carbonate chemistry of seawater. Here we use both sediment trap and box core samples from the Santa Barbara Basin to evaluate the relationship between the calcification intensity of the planktonic foraminifera species *Globigerina bulloides*, measured by area density (μg/μm^2), and the carbonate ion concentration of seawater ([CO_3^{2-}]). We also evaluate the influence of both temperature and nutrient concentration ([PO_4^{3-}]) on foraminiferal calcification and growth. The presence of two *G. bulloides* morphospecies with systematically different calcification properties and offset stable isotopic compositions was identified within sampling populations using distinguishing morphometric characteristics. The calcification temperature and by extension calcification depth of the more abundant "normal" *G. bulloides* morphospecies was determined using $\delta^{18}O$ temperature estimates. Calcification depths vary seasonally with upwelling and were used to select the appropriate [CO_3^{2-}], temperature, and [PO_4^{3-}] depth measurements for comparison with area density. Seasonal upwelling in the study region also results in collinearity between independent variables complicating a straightforward statistical analysis. To address this issue, we use additional statistical diagnostics and a down core record to disentangle the respective roles of each parameter on *G. bulloides* calcification. Our results indicate that [CO_3^{2-}] is the primary variable controlling calcification intensity while temperature influences shell size. We report a modern calibration for the normal *G. bulloides* morphospecies that can be used in down core studies of well-preserved sediments to estimate past [CO_3^{2-}].

1. Introduction

Planktonic foraminifera are ubiquitous microzooplankton that secrete calcium carbonate ($CaCO_3$) shells that comprise up to 80% of the calcite preserved in seafloor sediments [*Schiebel*, 2002]. Fossil shells of foraminifera preserved in marine sediments have been used for a wide variety of paleoclimate applications that have greatly enhanced our understanding of past oceanic and climatic conditions. Due to the relatively short life span of planktonic foraminifera (~1 month), their shells represent a brief snapshot of surface ocean conditions during their time of calcification [*Bé*, 1977]. It is generally accepted that surface ocean carbonate ion concentration ([CO_3^{2-}]) plays a key role in the calcification of planktonic foraminifera with the level of response varying among species [e.g., *Spero et al*., 1997; *Bijma et al*., 1999, 2002; *Barker and Elderfield,* 2002; *Mekik and Raterink,* 2008; *Moy et al*., 2009; *Marshall et al*., 2013]. The calcification intensity of planktonic foraminifera, or the amount of calcite deposited relative to shell size, reflects both the efficiency (effort to precipitate calcite under varying environmental conditions) and the rate (how much calcite is added over time) of calcification during an individual's lifespan [*Weinkauf et al*., 2016]. Calcification intensity of fossil foraminiferal shells can be estimated using morphometric characteristics such as weight, size, and area.

Initial morphometric observations of shells grown in culture and their relationship to carbonate chemistry indicate that the species *Orbulina universa* produced a 37% higher shell mass at elevated [CO_3^{2-}] (600 μmol kg^{-1}) relative to that of individuals grown in ambient seawater [CO_3^{2-}] (170 μmol kg^{-1}) [*Spero et al*., 1997; *Bijma et al*., 1999, 2002]. Subsequently, *Barker and Elderfield* [2002] found that the size-normalized shell weights (SNSW), which are more reflective of shell thickness rather than size, from a series of core-top samples varied systematically with latitude. The authors found that SNSW decreased with increasing latitude due to increased CO_2 solubility and declining [CO_3^{2-}] associated with decreasing temperature [*Barker and*

Elderfield, 2002]. A down core study in the Southern Ocean observed that SNSW of postindustrial age foraminiferal shells from surface sediments were 35% lower than Holocene age shells and attributed this difference to increasing anthropogenic CO_2 and declining [CO_3^{2-}] during the last two centuries [*Moy et al*., 2009]. A recent sediment trap study highlighted the importance of the shell weight size-normalization technique and described a new size-normalization method, area density, which resulted in a highly significant relationship with [CO_3^{2-}] for two species of tropical planktonic foraminifera [*Marshall et al*., 2013].

While considerable effort has gone into developing foraminiferal geochemical proxies for carbonate system variables [e.g., *Sanyal et al*., 1996; *Yu et al*., 2007; *Foster*, 2008; *Henehan et al*., 2013; *Rae et al*., 2011; *Allen et al*., 2011, 2012], relatively less emphasis has been placed on developing morphometric-based techniques [e.g., *Spero et al*., 1997; *Bijma et al*., 1999, 2002; *Barker and Elderfield,* 2002; *Marshall et al*., 2013]. In this regard, SNSW estimates of foraminiferal calcification intensity have great potential for serving as a quantitative measure for past [CO_3^{2-}]. SNSW analyses also require minimal analytical instrumentation and therefore can easily be measured in many laboratories. Because SNSW measurements are nondestructive, foraminifera used for this purpose can be used for geochemical analyses, thus providing tandem proxy records on a single sample population.

The development of proxy methods for estimating carbonate system parameters is needed since observational records are limited to the last 20–30 years [e.g., *Takahashi et al*., 1982; *Bates et al*., 2014]. Such methods could provide an indirect means for estimating how marine calcifiers and the marine carbonate system have responded to carbon perturbations on both short (decadal to century) and long time scales (millennial). These records would be instrumental in understanding how the marine carbonate system will respond to future increases in ocean acidification associated with various projected CO_2 scenarios. This study establishes a means to reconstruct past [CO_3^{2-}] by providing an empirical relationship between *Globigerina bulloides* calcification intensity and ambient [CO_3^{2-}] that can be applied to well-preserved marine sediments.

1.1. Variables Influencing Foraminiferal Growth and Calcification

The calcification and growth of planktonic foraminifera have been linked not only to seawater [CO_3^{2-}] but also to variables such as temperature and nutrient concentration [e.g., *Bé et al*., 1973; *Spero et al*., 1997; *Aldridge et al*., 2012]. It has been suggested that a unique combination of these factors comprises a species-specific set of "optimal growth" conditions that result in a stress-induced, reduced calcification response when these environmental conditions are not satisfied [*de Villiers*, 2004]. However, several tests of the optimal growth hypothesis failed to find a link between either the absolute abundance of a given species, which would hypothetically occur under that species' optimal growth conditions, or the calcification intensity of those individuals [*Beer et al*., 2010a; *Weinkauf et al*., 2013, 2016]. Rather, a study using Mediterranean sediment samples indicated that the calcification of four species of planktonic foraminifera responded passively to changes in seawater properties, such as [CO_3^{2-}], as opposed to a physiologic response brought about by stress from unfavorable conditions [*Weinkauf et al*., 2013]. Despite being unable to identify the specific environmental factors that controlled calcification response for each of these species, the results of this work were consistent with carbonate chemistry being the primary control on calcification [*Weinkauf et al*., 2013]. Furthermore, another study evaluated foraminiferal calcification change over a deglaciation (Marine Isotope Stages 6-7) and noted that *Globigerinoides ruber* and *G. bulloides* showed very similar calcification responses despite having very different ecological requirements and therefore optimal growth conditions. Rather, these changes were linked to pCO_2 and the carbonate saturation of seawater [*Gonzalez-Mora et al*., 2008].

Temperature has been cited as a control of foraminiferal shell size, with larger shells growing in warmer waters [*Bé et al*., 1973; *Hecht*, 1976; *Schmidt et al*., 2004; *Lombard et al*., 2009], where [CO_3^{2-}] is also generally high. In order to differentiate the influence of these variables, a culture study by *Lombard et al.* [2010] maintained constant temperature and varied [CO_3^{2-}] and observed that foraminifera (*Orbulina universa* and *Globigerinoides sacculifer*) had a significant increase in shell weight with no significant change in shell size in response to elevated [CO_3^{2-}]. This result corroborated earlier observations of lower SNSW associated with the Holocene relative to SNSW during the Last Glacial Maximum when temperatures were colder and [CO_3^{2-}] was higher [*Barker and Elderfield*, 2002]. While previous results indicate that [CO_3^{2-}] is the predominant factor

controlling calcification intensity, some research has suggested that temperature does perhaps play an important role in calcification rate, which is inherently related to calcification intensity. A study of eight modern planktonic foraminifera species found that increased temperature resulted in an increase in calcification rate across all species [*Lombard et al*., 2009]. *de Villiers* [2004] also concluded that optimum temperatures were an important factor in foraminiferal calcification rates measured by SNSW. Contrary results from a culturing study by *Manno et al.* [2012] indicated that increased temperature resulted in no net change in *Neogloboquadrina pachyderma* (sinistral) calcification rate. Rather, this study found that a decline in pH and by extension [CO_3^{2-}] resulted in a significant decline in calcification rate even in cultures where temperature was elevated simultaneously.

Due to the fact that previous results indicate that shell size is influenced by temperature, size normalization of shell weights is essential for creating a metric that best constrains calcification intensity [e.g., *Barker and Elderfield*, 2002; *Lombard et al*., 2010; *Beer et al*., 2010a]. Sieve-based weights (SBW), measurement-based weights (MBW), and area density (AD) are examples of such methods. SBW measurements are made on a narrow size range (~50 μm) by sieving and measuring the mean weight of a pool of individuals to calculate an average weight for the sample population [*Broecker and Clark*, 2001]. MBW more effectively account for shell size by normalizing sieve-based weights with a mean diameter or silhouette area parameter [*Barker and Elderfield*, 2002]. However, both of these size-normalizing methods are confined to examination of a narrow size fraction of sediments, thereby potentially limiting the number of individuals available for analysis (see *Marshall et al*. [2013] for a review). Area density overcomes this limitation by using an individual rather than a population approach, allowing for a broad size fraction to be used and maximizing the number of individuals available per sample [*Marshall et al*., 2013]. The area density method uses an individual weight and silhouette area measured for each shell and normalizes individual weights prior to taking the population mean. Although time consuming, the area density method effectively captures the intrinsic natural variability of biological samples, particularly at the individual level that would otherwise be lost when measuring bulk weights. Furthermore, since there is no size-fraction restriction for the AD method, a larger number of individuals are typically available for analysis, thus generating a more robust estimate of the sample population. Importantly, the area density method has also proven to be the most effective size-normalization technique, which is important in calcification intensity studies such as this one [*Beer et al*., 2010b; *Marshall et al*., 2013].

While temperature and [CO_3^{2-}] have been the primary variables considered in foraminiferal calcification studies, some research indicates that nutrient concentration may also influence foraminiferal calcification. A North Atlantic study of the species *G. bulloides* suggests that high concentrations of nitrate (NO_3^-) and phosphate (PO_4^{3-}) have adverse effects on calcification of this species [*Aldridge et al*., 2012]. Previous research on corals and coccolithophores has observed a decline in calcification as a result of high nutrient concentrations, which is attributed to adsorption of calcium hydrogen phosphate ($CaHPO_4$) onto the calcite surface blocking growth cites for crystallization [*Kinsey and Davies,* 1979; *Paasche and Brubank,* 1994; *Lin and Singer,* 2006]. Conversely, the results of a sediment trap study in the Cariaco Basin (Venezuela) indicate that nutrients are not a key factor controlling calcification intensity of two planktonic foraminiferal species (*G. ruber* and *G. sacculifer*) and that covariation between [CO_3^{2-}] and nutrient concentrations can result in spurious correlations between foraminiferal calcification intensity and nutrient concentration [*Marshall et al*., 2013].

2. Regional Setting: The Santa Barbara Basin

This study utilizes *G. bulloides* shells preserved in marine sediments (both sediment trap and sediment core) and hydrographic data collected off the California Margin in the Santa Barbara Basin (SBB). *Globigerina bulloides* is a species that often dominates the foraminiferal flux in the SBB [*Kincaid et al*., 2000] and has been used commonly in down core paleoceanographic reconstructions for this basin [e.g., *Hendy and Kennett,* 1999; *Friddell et al*., 2003; *Pak et al*., 2004, 2012]. It is a symbiont-barren spinose foraminifera found in transitional to subpolar waters and is frequently found in association with upwelling regimes [*Bé*, 1977; *Hemleben et al*., 1989].

The SBB is an approximately 100 km long, ~600 m deep east-west trending basin extending from Point Conception to the greater Los Angeles area (Figure 1). There are north and south bounding continental shelves, with the Channel Islands forming the southern bound of the basin. Sills at the eastern and western mouths of the basin (200 m and 400 m, respectively) restrict water exchange between the basin and the open

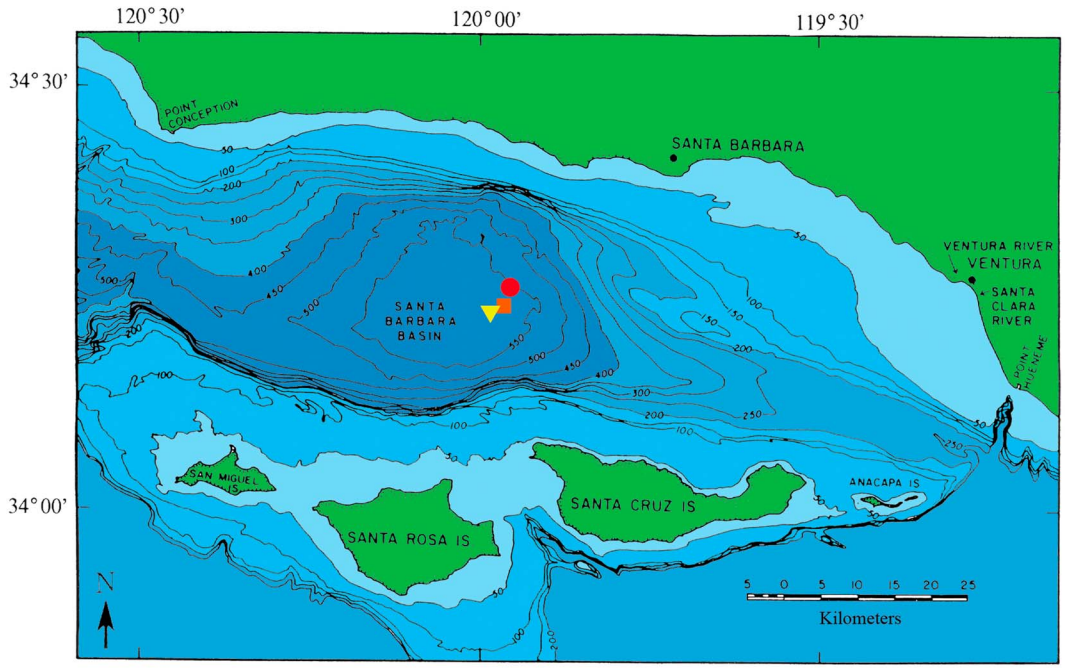

Figure 1. Bathymetry of the Santa Barbara Basin with the location of the sediment trap mooring (yellow triangle), Plumes and Blooms Station 4 (orange square), and box core (red circle).

ocean. Limited influx of oxygenated water coupled with high productivity rates result in anoxic conditions in the deepest part of the basin producing ideal conditions for the preservation of annually laminated or varved sediments [*Reimers et al*., 1990; *Thunell et al*., 1995]. Prevailing southward winds result in Ekman-induced upwelling in the basin that typically peaks during the spring to early summer months and relaxes during the fall and winter [*Hendershott and Winant*, 1996]. Seasonal upwelling produces a wide range of [CO_3^{2-}], temperature, and nutrient values, making this an ideal setting for examining the influence of each of these variables on calcification (Figure S1 in the supporting information).

3. Materials and Methods

3.1. Sediment Trap and Sediment Core Samples

The University of South Carolina has maintained a sediment trap time series in the deepest portion of the SBB (34°14′N, 120°02′W, ~580 m water depth; Figure 1) from 1993 up to present [*Thunell et al*., 1995, 2007; *Thunell*, 1998]. McLean Mark VII-W automated sediment traps equipped with 0.5 m^2 funnel openings are deployed for 6 month periods and samples are collected continuously on a biweekly basis. Sample bottles are buffered and poisoned with a sodium azide solution prior to deployment. Sediment samples are split using a McLean four-head rotary splitter and usually refrigerated in sodium borate buffered deionized water to prevent dissolution of carbonates prior to sample use. This study utilizes sediment trap material collected from 2007 to 2010, a period when water column carbonate system variables were measured on water samples collected near the SBB sediment trap mooring by the Plumes and Blooms Program.

Additionally, a 0.5 m box core collected in 2012 near the sediment trap mooring (34°13′N, 119°58′W, 580 m water depth; Figure 1) was used to supplement our sediment trap observations. Radiogenic isotopes of lead (^{210}Pb) and cesium (^{137}Cs) were used to develop an age model for the box core (Texts 1 in the supporting information) using a high-purity germanium well detector [*Moore*, 1984]. Radioisotope activities indicate an average sedimentation rate of 0.43 cm yr^{-1}; and an average mass accumulation rate of 5.84 g cm^2 yr^{-1} (Figure S2 in the supporting information). Using these age constrains, we estimate that the 0.5 m core extends back to ~1895 and the uppermost sediments contained in the core represent the year ~2006.

A 1/16 split of each sediment trap sample and roughly 3 g of box core sediment were used for foraminiferal analyses; if insufficient material was available from the sediment trap sample, an additional 1/16 split was used. Despite the high organic matter content typically found in sediment trap samples, previous tests demonstrated that an oxidative treatment of the samples (buffered 30% H_2O_2 for 45 min) yielded statistically identical area density values to that of untreated samples [*Marshall et al*., 2013]. Therefore, it was deemed unnecessary to oxidatively clean sediment trap samples prior to area density analysis. Both trap and core sediments were washed using borate buffered deionized water through a 125 μm sieve and dried in a 40°C oven prior to analyses.

3.2. Hydrographic Measurements

Monthly hydrographic measurements are made along a transect in the SBB by the Plumes and Blooms Program (http://www.icess.ucsb.edu/PnB/PnB.html), with one of the sampling stations (Station 4; 34°15′N, 119°54′W) located adjacent to the sediment trap mooring (Figure 1). From 2007 to 2010 total alkalinity (TA) and total dissolved inorganic carbon (DIC) measurements were also made at Station 4 on 25 monthly cruises that took place over a 40 month period (Text S2 in the supporting information). Water samples used for TA and DIC analyses were collected at depths of 0, 5, 10, 20, 30, 50, 75, 100, 150, and 200 m.

The CO2Sys program (version 2.1) originally by *Lewis and Wallace* [1998] (CO2SYS.BAS) and modified by *Pierrot et al.* [2006] was used to estimate unknown seawater marine carbonate system variables. This program uses two "master" carbonate system variables (TA, DIC, pH, and pCO_2) to estimate the remaining unknown variables at a set of given input conditions (e.g., temperature, salinity, and pressure). For the time period associated with the sediment trap samples (2007–2010), [CO_3^{2-}] is estimated using in situ measurements of TA and DIC from the SBB. Supplementary CTD and bottle data from Plumes and Blooms Station 4 including salinity, temperature, pressure, phosphate concentration ([PO_4]), and silicate concentration ([SiO_4]) are used as input conditions for these calculations. For the sediment core portion of the study, pCO_2 and TA are used as mater variables. We assume a constant TA of 2250 μmol kg^{-1} based on the mean measured surface TA measured in the SBB from 2007 to 2010. Seawater pCO_2 is derived according to Henry's Law using atmospheric CO_2 measurements from the Mauna Loa time series (1960 up to present; http://www.esrl.noaa.gov/gmd/ccgg/trends/) and temperature-, salinity-, and pressure-dependent solubility coefficients (K_0) following the formulation of *Weiss* [1974]. Measured sea surface temperature from the SBB (1955 up to present; 34°24.2′N, 119°41.6′W″) and salinity from the Scripps Pier (1916 up to present; 32°52.0′N, 117°15.5′W) measured as a part of the Shore Stations Program (http://shorestations.ucsd.edu/shore-stations-data/) were used to determine time-specific K_0 values and as input conditions for our down core calculations. The dissociation constants (K_1 and K_2) determined by *Mehrbach et al.* [1973] and refit to the seawater scale by *Dickson and Millero* [1987] were used as constants for our CO2Sys carbonate system calculations. The HSO_4 and $B(OH)_3$ dissociation constant (K_{SO4} and K_B, respectively) according to *Dickson* [1990] and the boron concentration and chlorinity relationship determined by *Lee et al.* [2010] were used for our calculations.

3.3. Area-Normalized Shell Weights: The Area Density Method

A total of 82 sediment samples (39 sediment trap and 43 sediment core) are included in our area density analysis. We use a combination of upper and lower sediment trap samples ($n = 32$) that coincide with the 25 TA and DIC sampling periods (2007–2010) for our modern area density sediment trap calibration. Lower trap samples (~450 m depth) were available for 22 of the 25 carbonate chemistry sampling periods, while upper trap samples (~150 m depth) were available for 10 of these periods. The upper sediment trap was added to the SBB sediment trap mooring in 2009 allowing for both upper and lower sediment trap samples to be analyzed for eight of the TA and DIC sampling periods. An additional seven sediment trap samples from months when no water column carbonate chemistry data are available were analyzed to produce a full annual cycle of area density measurements from December 2009 to December 2010.

Globigerina bulloides shells were systematically picked from the >125 μm size fraction of each sediment sample using a gridded tray. The >125 μm size fraction was chosen because *G. bulloides* smaller than this range likely represent individuals that have not reached the adult stage [*Berger*, 1971; *Peeters et al*., 1999]. On average shell diameters from sediment trap and core samples range from 200 to 400 μm in size. Atypical *G. bulloides* shells with abnormally large and thin final chambers or individuals with oversized apertures where the final chamber is not fully sutured to the test were excluded from our analyses due to the

effect these morphologic features have on shell area. Careful attention was paid to selecting individuals that were free of visible clay particles or organic matter that could potentially bias shell weights.

SNSW were measured using the area density method described in detail by *Marshall et al.* [2013]. Following this method, individual shells were weighed in a copper weigh boat using a high-precision microbalance (Mettler Toledo XP2U; ±0.43 μg) in an environmentally controlled weigh room and then photographed umbilical side up using a binocular microscope (Zeiss Stemi 2000-C) fitted with a camera (Point Grey Research Flea3 1394b). Photos were uploaded to a microscopic imaging program (Orbicule Macnification 2.0) to measure the length of the longest shell diameter (Feret diameter) and the 2-D surface area or silhouette area of each shell. This program uses RGB images to calculate a region of interest by outlining the imaged shell to estimate a pixel 2-D area. Pixel measurements are converted to lengths (μm) and areas (μm^2) by calibrating an image of a 1 mm microscale taken at the same magnification and working distance as shell photos. Individual weights were then divided by their corresponding areas, and the mean area density value was calculated for each sample population (equation (1)). Mean area density values are most representative of the population calcification intensity and by extension ambient calcification conditions and were the focus of our calibration and statistical analyses. Ideally, 40 individuals were included in each sample population in order to minimize measurement standard error ($SE = \sigma/\sqrt{n}$). Due to the asymptotic nature of area density standard error, we would argue that a sample size of 30–40 individuals represents a high level of confidence (Figure S3 in the supporting information).

$$\text{area density}\left(\mu g/\mu m^2\right) = \text{individual weight}(\mu g)/\text{individual area}\left(\mu m^2\right) \quad (1)$$

3.4. Stable Isotope Analysis

Approximately 70 μg (15–30 individuals) of *G. bulloides* from each sample used for area density analyses were pooled to measure $\delta^{18}O$. The foraminifera were cleaned for 30 min in 3% H_2O_2 followed by a brief sonication and acetone rinse. Isotopic analyses were carried out on an Isoprime isotope ratio mass spectrometer equipped with a carbonate preparation system. The long-term standard reproducibility is 0.07‰ for $\delta^{18}O$. Results are reported relative to Vienna Pee Dee Belemnite (V-PDB). Because the $\delta^{18}O$ of foraminifera reflects both seawater temperature and the $\delta^{18}O$ of seawater ($\delta^{18}O_w$), accounting for any variations in $\delta^{18}O_w$, is essential to properly estimating temperature. The $\delta^{18}O_w$ varies as a function of salinity, and therefore, a $\delta^{18}O$:salinity relationship typically is used to determine $\delta^{18}O_w$; here we use a $\delta^{18}O$:salinity relationship that was determined specifically for the Southern California Bight (equation (2)). Measured sea surface salinity from Plumes and Blooms (Station 4) and the SIO Pier time series (1916 up to present) are used, respectively, for sediment trap and sediment core estimates of $\delta^{18}O_w$. The use of measured surface salinity as opposed to assuming constant salinity for the down core record was particularly important in calculating $\delta^{18}O_w$ and the resulting temperature estimates. Scaling to V-PDB from standard mean ocean water (SMOW) of estimated $\delta^{18}O_w$ was done by subtracting 0.27‰ [*Hut*, 1987]. $\delta^{18}O$ calcification temperatures were calculated using a culture-derived temperature relationship (equation (3)) developed within the Southern California Bight region for *G. bulloides* (12-chambered shells) [*Bemis et al.*, 1998].

$$\delta^{18}O_{water} = 0.39*(\text{salinity})-13.23 \quad (2)$$

$$T(°C) = 13.2-4.89*\left(\delta^{18}O_{calcite} - \delta^{18}O_{water}\right) \quad (3)$$

4. Results and Discussion

4.1. Comparison of Sediment Trap and Sediment Core Area Density Measurements

Assessing the potential for dissolution of foraminiferal shells within the water column and on the seafloor is of utmost importance when using foraminiferal shell weights as a water column proxy. For a total of eight sampling periods from 2009 to 2010, samples from both trap depths were available for area density analysis and are used to assess similarities and differences of area density and morphometric measurements recorded at each sampling depth. A comparison of measurements from each depth was used to determine if dissolution impacts foraminiferal shells as they settle through the water column, and a comparison of sediment trap and sediment core measurements is used to assess the potential for seafloor dissolution.

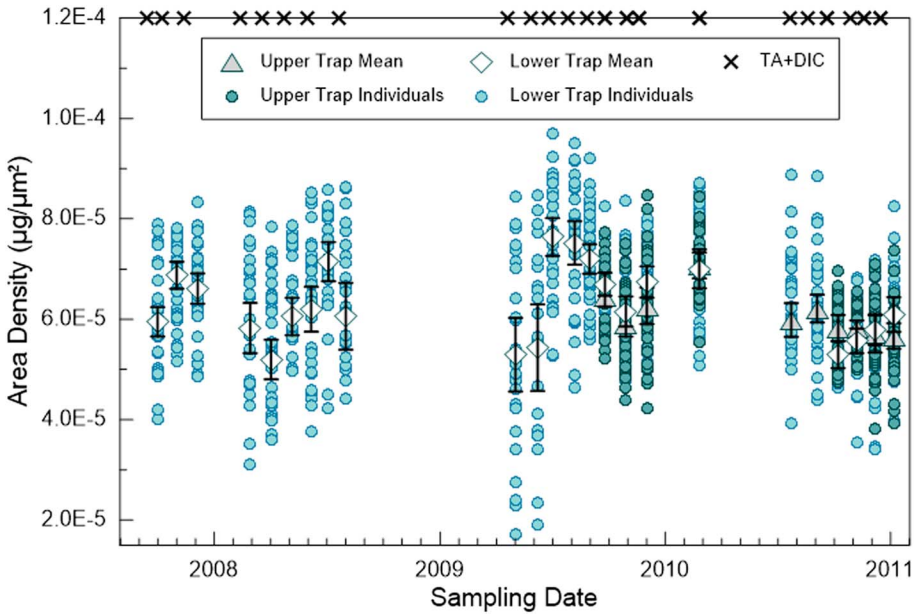

Figure 2. Discontinuous time series of normal *G. bulloides* mean area density from upper (triangles) and lower (diamonds) sediment trap samples and the spread of the individual measurements included in each sample mean (circles). Error bars represent two standard errors of the sample means. Hydrographic sampling of TA and DIC are indicated by "crosses" on the *x* axis.

Observations by *Milliman et al.* [1999] suggest that 60–80% of $CaCO_3$ particles dissolve in the upper 500–1000 m of the water column despite being well above the lysocline. The mechanism driving water column dissolution is not well understood and has not been replicated by either in situ [*Thunell et al.*, 1981] or modeling studies [*Jansen et al.*, 2002]. Estimates for the Pacific Ocean north of 20°N indicate that the depth of the calcite saturation horizon can range from 200 to 1000 m with a mean of 600 m water depth [*Feely et al.*, 2004]. Water column measurements of TA and DIC from 2007 to 2010 in the SBB were used to assess calcite saturation. Although water column measurements are limited to 0–400 m, these data indicate supersaturated values (1.25) at 400 m and suggest that supersaturation also exists at the basin bottom (600 m water depth; Figure S4 in the supporting information). The preservation of unfragmented assemblages of foraminifera and the occasional presence of aragonite thecosome pteropods that are highly susceptible to dissolution are physical evidence that preservation of calcite in the SBB is not an issue. Shell features that are typically used as indicators of dissolution, such as reduced spine bases and formation of cracks [*Dittert and Henrich,* 2000], are not observed in trap or core sediments.

For the eight sampling periods where both upper and lower trap samples were measured, the mean area density values determined for each depth are within two standard errors of each other (Figure 2). Independent *t* tests indicate that there is no significant difference in the area density population means for six of eight sampling periods (p 2 tail > 0.05), while there is a moderately different sample mean recorded for a single sampling period (p 2 tail $= 0.02$; 25 September 2009) and a significant different sample mean for one sampling period (p 2 tail < 0.001; 8 October 2010). These results indicate that generally there is no difference in area density between the two sampling depths suggesting that there is no significant dissolution occurring within the SBB water column.

We also compare shell weights, diameters, and area densities between the sediment trap and the seafloor sediments to assess postdepositional dissolution. If significant dissolution is occurring on the seafloor in SBB, we would expect to see differences in shell morphometric characteristics in the sediment trap samples versus the seafloor samples. While the lack of temporal overlap between sediment trap (2007 to 2010) and down core measurements (1985–2005) is not ideal for such a comparison, measurements from each of these populations indicate a similar range in weight and size. Independent *t* tests were conducted to statistically determine if the weight, diameter, and area density of shells collected by the trap and in the core are significantly different. These results indicate there is no significant difference in shell size preserved in trap and

seafloor sediments ($p > 0.05$). However, there is a moderately significant difference in shell weight ($p > 0.01$) and highly significant difference in area density ($p < 0.001$). The results of this comparison indicate that overall higher weights and area density values are observed in core sediments relative to trap sediments. We attribute these offsets to higher [CO_3^{2-}] and increased calcification intensity over the 100 year down core sampling period relative to the more recent sediment trap sampling period (See section 4.6 for discussion on [CO_3^{2-}] change over this interval).

4.2. *Globigerina bulloides* Morphospecies

Studies of *G. bulloides* small subunit ribosomal RNA (SSU rRNA) indicate high cryptic diversity with a total of seven distinct genotypes [*Darling and Wade*, 2008]. Genetic studies of *G. bulloides* from the SBB and the greater Southern California Bight have identified the presence of two of these genotypes that represent two distinct morphospecies [*Darling et al*., 2000]. The most dominant genotype, IId, is found in abundance throughout the year, while a rare genotype, IIa, which is found commonly at high latitudes, is present during cool periods in the SBB [*Darling et al*., 1999, 2000, 2003]. It was speculated that the IIa individuals were a heavily calcified *G. bulloides* morphotype that has previously been observed in the Southern California Bight [*Darling et al*., 2003]. *Sautter and Thunell* [1991a] first identified a heavily calcified "encrusted" morphotype of *G. bulloides* that is enriched in ^{18}O during peak upwelling (April) in the San Pedro Basin, located just south of the SBB. *Hendy and Kennett* [2000] also identified an abundant small and thickly calcified *G. bulloides* morphotype in glacial sediments from the SBB. *Bemis et al.* [2002] applied a $\delta^{18}O$ temperature relationship derived for normal *G. bulloides* to these encrusted glacial specimens and found that they yielded unreasonably cold temperature estimates.

Due to the fact that species- and morphospecies-specific calcification responses have been documented in foraminifera, it is important to determine if more than one *G. bulloides* morphospecies exists in our sample populations and if these morphospecies calcify differently. Since both genetic observations and isotopic analyses of *G. bulloides* morphospecies within the SBB indicate two distinct forms, it is likely that these morphospecies also calcify differently [*Bemis et al*., 2002; *Darling et al*., 2003]. To assess if calcification varies between encrusted (IIa) and "normal" *G. bulloides* (IId), we examined weight-area and area density-diameter relationships of individuals included in our study. *Marshall et al.* [2015] demonstrated that cryptic species of *Orbulina universa* can be identified using this technique and highlighted significant differences in calcification between morphospecies in the Cariaco Basin, Venezuela.

If the calcification differs between morphospecies, we would expect the slopes and intercepts of their weight-area regressions to be different. We would also expect to see a distinct grouping of morphotype populations when area density is regressed against shell diameter with the encrusted individuals likely plotting in the higher-area density range. This assessment indicates that the encrusted *G. bulloides* morphotype is present in our samples and does in fact calcify differently from the normal morphotype. The weight-area relationship of the less abundant encrusted morphotype has a slightly higher intercept and a steeper slope (Figure S5 in the supporting information). Encrusted individuals identified by our weight-area analyses were also identified using area density-diameter relationships, with the encrusted individuals plotting in the upper area density range. Accordingly, these morphometric relationships were used to identify encrusted individuals, and we exclude them from our normal sample populations.

The normal *G. bulloides* morphospecies dominates all sample populations with typically fewer than two encrusted individuals in each sample. However, during winter and peak upwelling periods the abundances of encrusted individuals increase and comprise as much as 15–25% of the *G. bulloides* population. The association of the encrusted *G. bulloides* with cooler conditions is not surprising due to the fact that this genotype is found typically in polar regions [*Darling et al*., 2003]. For a limited number of samples there were enough individuals of the encrusted form to compare mean area densities between the two morphospecies. The difference between normal and encrusted populations is illustrated by plotting mean area density versus mean size-normalized shell weight (mean sample weight/mean sample diameter) (Figure 3). The encrusted morphospecies consistently have a higher weight and area density range due to the more heavily calcified nature of their shells.

It is important to note that not all encrusted individuals identified by our weight-area analyses were visually distinct using a light microscope. A closer evaluation of surface texture and pore density of the two

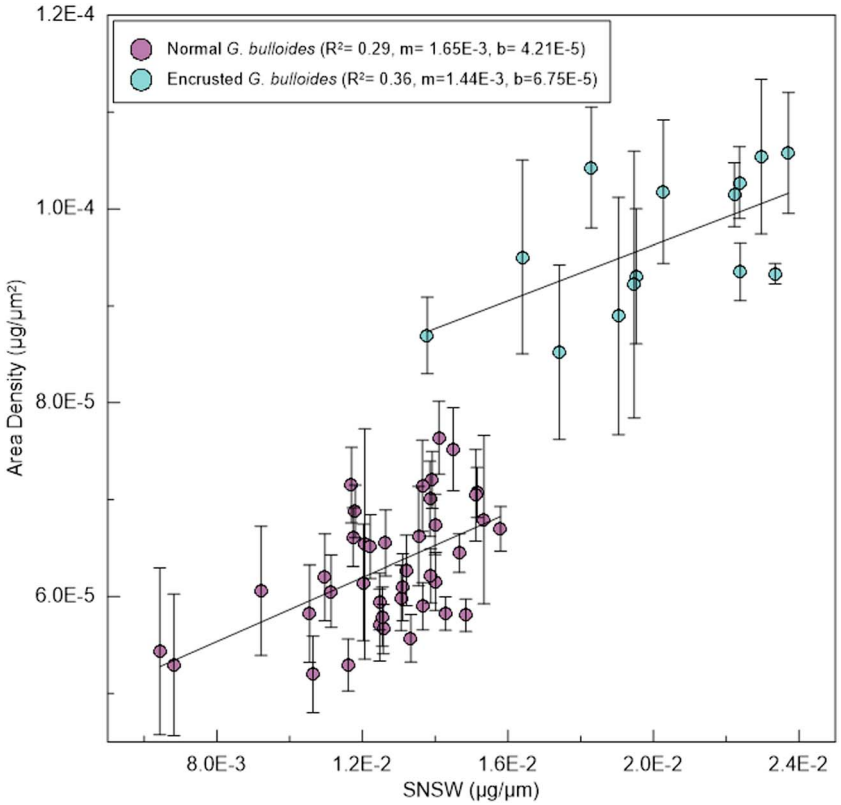

Figure 3. Comparison of area density-SNSW of the normal and encrusted morphospecies included in our study. SNSW were determined for each sample by taking the mean sample weight and dividing by mean sample diameter. Error bars represent the two standard errors of each sample population ($SE = 2\sigma/\sqrt{n}$).

morphotypes using a scanning electron microscope (SEM) reveals a decreased pore density and more rigid surface structure of encrusted compared to normal *G. bulloides* (Figure 4). While previous studies have suggested that encrusted *G. bulloides* are rare in the Southern California Bight, possibly due to the difficulty of visual distinction between the morphospecies, our results indicate that this morphospecies is more abundant

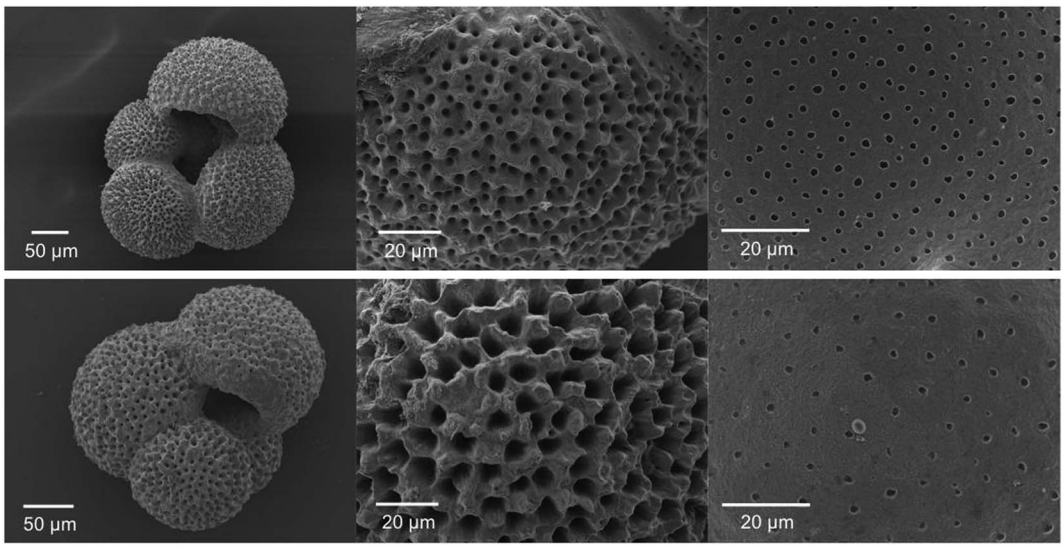

Figure 4. SEM images of (top row) normal and (bottom row) visually distinct encrusted whole shells, external surface textures, and pore density imaged from the inner shell wall.

than previously thought. Frequency distributions of individual morphometric measurements (shell diameter, weight, 2-D area, and area density) from the entire sediment trap data set for normal ($n = 1108$) and encrusted ($n = 77$) *G. bulloides* were used to identify characteristic features of each morphospecies (Figure S6 in the supporting information). These data indicate that the morphospecies are similarly sized, although encrusted individuals are slightly smaller in terms of diameter and 2-D area and are typically heavier although the ranges in weights between morphospecies overlap making this a nondiagnostic characteristic. The difference in area density distributions between morphospecies is the most diagnostic feature for differentiating the normal and encrusted morphospecies. Based on this assessment, the combination of a weight and size measurement is the best morphological means to confidently differentiate between normal and encrusted *G. bulloides*. This method, as opposed to SEM analyses that require sample coating, is particularly useful if individuals will be used later for geochemical analyses.

4.3. δ^{18}O-Derived Calcification Depths

Previous sediment trap and plankton tow studies have verified that the δ^{18}O of *G. bulloides* is a reliable indicator of the seawater temperature at which individuals calcified [*Curry and Matthews*, 1981; *Ganssen and Sarnthein*, 1983; *Kroon and Ganssen*, 1988; *Sautter and Thunell*, 1991b; *Thunell et al.*, 1999]. While we assume that the δ^{18}O value for multiple shells represents the mean temperature and depth at which each population of individuals calcified, there are limitations to this assumption. Single-specimen δ^{18}O results have shown that a considerable range of δ^{18}O can exist within a single sample population and this variability has been attributed to differences in depth habitats, bioturbation of sedimentary sequences, and possibly vital effects [*Killingley et al.*, 1981; *Ganssen et al.*, 2011]. A statistical assessment by *Schiffelbein and Hills* [1984] examined the relationship between the number of specimens used in a δ^{18}O analysis and measurement precision and recommended 20+ individuals for high confidence in bulk δ^{18}O measurements [*Schiffelbein and Hills*, 1984]. We used on average 20 individuals per δ^{18}O analysis in order to maximize confidence in our δ^{18}O values while preserving enough material to duplicate measurements. Another important consideration when using δ^{18}O to estimate calcification depth is that the δ^{18}O signature of foraminiferal calcite is a composite representation of various depth/calcification habitats throughout the life cycle of that individual. Although the exact depth habitats and timing of ontogenic stages are not well constrained, it is generally thought that juvenile planktonic foraminifera calcify in shallower water depths and that the majority of foraminiferal calcite is formed at greater depths within the water column during the final adult and terminal life stages [e.g., *Hemleben et al.*, 1989]. Lastly and perhaps most importantly for our study, bulk isotopic analyses may also include cryptic morphospecies. In our case the inclusion of encrusted *G. bulloides* that have a documented offset in their stable isotopic composition from the normal morphospecies can result in a δ^{18}O measurement that is a mixture of significantly different δ^{18}O end member values.

The oxygen isotopic composition of 15–30 individuals of *G. bulloides* was used to determine a mean calcification temperature (equation (3)) and by extension a mean calcification depth for each sediment trap sample. The depth of calcification was determined by comparing each population mean δ^{18}O calcification temperature to a time equivalent CTD temperature profile to determine the depth of that temperature. Anomalously high δ^{18}O (>0.80‰) from several winter and peak upwelling sampling periods were the first indication that ^{18}O-enriched encrusted individuals were included in some samples. A subsequent examination of weight-area relationships of the *G. bulloides* populations included in our initial stable isotope analyses supported this hypothesis. Duplicate measurements were made on sample populations that excluded encrusted individuals that were identified by morphometric analyses. For example, a stable isotope measurement on a sample from an upwelling period that included encrusted individuals had a δ^{18}O value of 0.66‰, equating to a calcification temperature of 8.2°C and an unreasonable calcification depth of greater than 200 m. A duplicate measurement made on a strictly normal population from the same sample yielded a δ^{18}O of −0.58‰, equating to a 14.3°C calcification temperature and a 20 m calcification depth. Morphometric analyses were used to identify and exclude initial δ^{18}O results from samples that included encrusted individuals. Duplicate δ^{18}O measurements where then made on strictly normal populations of *G. bulloides* from these samples. The stable isotope results indicate that normal *G. bulloides* calcifies over a range of temperatures and depths over the course of the 3 year time series ($n = 45$). δ^{18}O values range from 0.4 to −0.9‰, with a mean of −0.20‰.

Normal *G. bulloides* δ^{18}O temperatures estimated using equation (2) indicate a mean calcification temperature for *G. bulloides* of 12.5°C, with a range of 10–16°C. This range is in good agreement with the previously

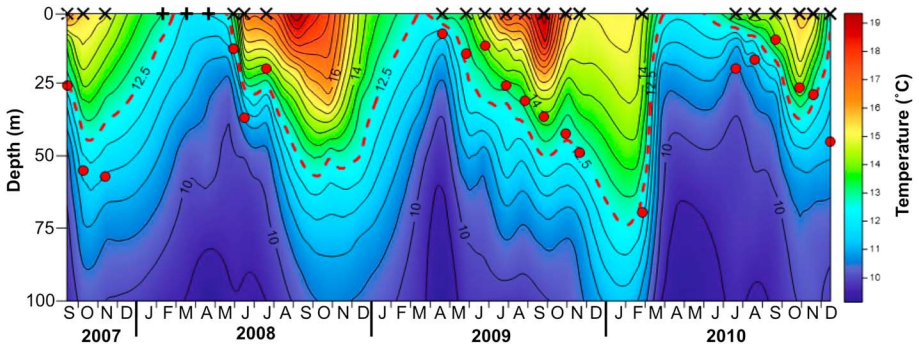

Figure 5. *G. bulloides* δ^{18}O derived calcification depths (red circles) plotted here with contoured measured temperatures (0–100 m) with the 12.5°C isotherm (dashed red) highlighted as the mean calcification temperature determined for this time series. This data set excludes three ^{18}O enriched samples from the strong upwelling period in 2008. The dates of coinciding hydrographic data are marked on the upper *x* axis as crosses with the three excluded samples marked by a "plus sign".

established preferred temperature range (11–16°C) for *G. bulloides* in this region [*Sautter and Thunell,* 1991a]. These results indicate that *G. bulloides* calcifies over a broad range of water depths (0–75 m), with a mean calcification depth of 40 m during the study period that loosely follows the 12.5°C isotherm. The range in calcification temperatures and depths is not surprising due to the fact that *G. bulloides* is a surface-mixed layer species whose depth habitat is influenced by seasonal upwelling and vertical migration of the thermocline and chlorophyll maximum [*Prell and Curry,* 1981; *Hemleben et al*., 1989; *Sautter and Thunell,* 1991a, 1991b]. Previous studies in upwelling regions have found *G. bulloides* at depths ranging from near the sea surface [*Thiede*, 1983; *Kroon and Ganssen,* 1988] to below the thermocline [*Fairbanks et al*., 1982]. Low δ^{18}O during upwelling suggests shoaling of the *G. bulloides* depth habitat during these periods. Generally, depth habitats and calcification temperatures tend to be deeper and cooler, respectively, prior to upwelling with a shift to shallower depths and warmer temperatures at the onset of upwelling (Figure 5).

Due to the range of δ^{18}O-determined calcification depths and the large surface to depth change in [CO_3^{2-}], temperature, and [PO_4^{3-}], the water column measurements were carefully selected to best reflect in situ calcification conditions before pairing with area density measurements. We use the δ^{18}O-derived calcification depth to select the applicable water depth measurement (0, 5, 10, 20, 30, 50, and 75 m). For three samples from an unusually strong upwelling period in early 2008, the very small sample sizes (smaller shells and lower abundances) did not allow for duplicate measurements to exclude encrusted individuals. Original δ^{18}O values indicate calcification temperatures less than 9°C and calcification depths well over 100 m. Encrusted individuals were identified using morphometric analyses and removed from the mean area density value for each of these samples, and the depth of the 12.5°C isotherm (mean calcification temperature) was instead used to assign a calcification depth.

4.4. Area Density Annual Cycle

Due to the discontinuous nature of the available carbonate chemistry data and the sediment trap samples selected for the area density:[CO_3^{2-}] calibration, seven additional sediment trap samples were measured to complete one full annual cycle of area density measurements from December 2009 to December 2010. Fourteen sediment trap samples were used to generate this continuous annual cycle of normal *G. bulloides* area density. Nine out of 14 samples had more than one encrusted individual; these individuals were removed from the normal population and are examined separately in our time series analysis. The Pacific Fisheries Upwelling Index (PFEL; http://www.pfeg.noaa.gov/products/PFEL; 33°N, 119°W), which is based on sea surface windstress, is used as an indicator of upwelling strength in SBB.

The highest area density values for both the normal and encrusted *G. bulloides* occur during winter months, when upwelling is weakest, and the lowest area density values generally occur during spring through early summer, when upwelling is strongest (Figure 6). We attribute the inverse relationship observed between *G. bulloides* area density and upwelling strength to the introduction of low [CO_3^{2-}] deep waters to the sea surface during periods of increased upwelling. The exact timing of changes in upwelling recorded by the PFEL index are reflective of sea surface conditions, while *G. bulloides* is responding to changes in upwelling

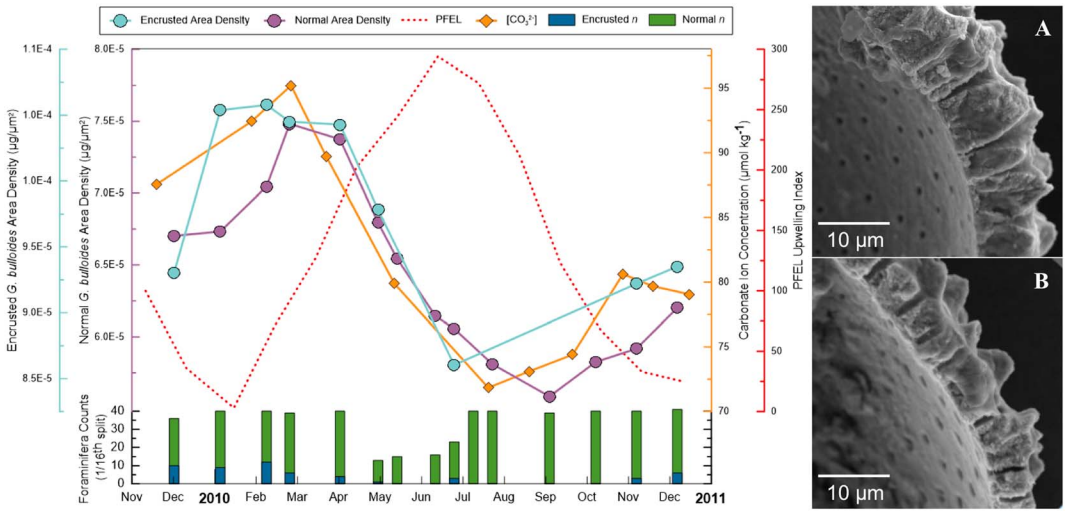

Figure 6. Normal and encrusted area density time series and 1/16th split abundance counts. The Pacific Fisheries Environmental Laboratory (PFEL) upwelling index is plotted as an indicator of upwelling strength, and estimates of in situ $[CO_3^{2-}]$ determined from measured temperature and oxygen indicate shifts in $[CO_3^{2-}]$; SEM images illustrate the difference in shell wall thickness from a (a) nonupwelling sample and an (b) upwelling sample.

that occur at varying depths within the water column. Generally, the $\delta^{18}O$-derived calcification depth of normal *G. bulloides* remains around 40–50 m with the exception of upwelling. During peak upwelling in March the calcification depth shoals to the surface mixed layer, and when upwelling weakens in April the calcification depth deepens to 25 m. Because TA and DIC measurements were not made continuously over this interval, we use measured temperature and oxygen concentration from the Plumes and Blooms and CalCOFI data sets to estimate $[CO_3^{2-}]$ using an empirical relationship relating these two variables [*Alin et al.*, 2012]. Changes in $[CO_3^{2-}]$ agree well with the seasonal trends observed in both normal and encrusted area densities (Figure 6). SEM images of final chamber shell wall cross sections taken of similarly sized individuals from a peak upwelling and nonupwelling period clearly illustrate differences in shell wall thickness associated with low and high $[CO_3^{2-}]$ conditions, respectively (Figures 6a and 6b).

We also evaluated how abundances of encrusted and normal *G. bulloides* vary in relation to seasonal hydrographic changes in the SBB. The number of encrusted and normal individuals was determined for a 1/16 split of each sample, with the maximum number of individuals picked from any sample being 40 (Figure 6). Four consecutive sediment trap samples extending from late April to late June had fewer than 40 normal *G. bulloides* in a split, with the lowest number of individuals (13) occurring in April, coinciding with the lowest temperatures and strongest upwelling (Figure 6). Interestingly, the timing of the lowest normal *G. bulloides* abundances does not coincide with the lowest area densities. Several other studies have also indicated that calcification intensity and abundance of *G. bulloides* are not always linked, weakening the optimal growth hypothesis proposed by *de Villiers* [2004] *Beer et al.* [2010a]; *Weinkauf et al.* [2013]. The lack of synchroneity between lowest abundance, which would hypothetically coincide with the species' nonoptimal growth conditions, and lowest calcification intensity instead suggests that *G. bulloides* calcification is responding abiotically to changes in its calcification environment as proposed by *Weinkauf et al.* [2013], while abundance is responding to favorable ecological conditions.

While *G. bulloides* has generally been identified as an "upwelling indicator," peak abundances of the normal morphospecies in the SBB are inversely related to upwelling strength. These observations suggest that normal *G. bulloides* thrive when the mixed layer is deep, the water column is well stratified, and there is a well-defined chlorophyll maximum. Such conditions exist during the nonupwelling periods in the fall and winter months in the SBB. Like normal *G. bulloides*, the encrusted form was not only found in highest abundance during winter months but also reappears briefly during peak upwelling in late May. Peak abundances of the encrusted morphospecies also occur during nonupwelling periods, but there is also a considerable secondary pulse of encrusted individuals that coincides with peak upwelling, indicating that this morphospecies thrives in low-temperature conditions.

There were enough encrusted individuals to evaluate the stable oxygen and carbon isotopic composition of this morphospecies from four samples used in the area density time series. Encrusted samples are consistently enriched in both ^{13}C and ^{18}O relative to values determined for time-equivalent normal individuals. Our analyses indicate that on average there is a 0.5‰ and a 1.0‰ offset between the $\delta^{18}O$ and $\delta^{13}C$, respectively. However, there is considerable variability in offsets, particularly for $\delta^{18}O$. Therefore, due to the limited number of observations ($n = 4$) these average offsets should be considered with caution. When the normal $\delta^{18}O$-temperature calibration is applied to encrusted samples, the resulting temperature estimates are up to 2°C colder than those for the normal individuals, resulting in calcification depth estimates that differ by nearly 100 m.

4.5. Regression Analysis

A series of regression analyses (simple, multiple, and hierarchical) were conducted using SPSS statistical software (IBM) to test the correlations between water column variables (in situ [CO_3^{2-}], temperature and [PO_4^{3-}]) and normal *G. bulloides* mean shell area density (Text S3 in the supporting information). Statistical analyses were also used to evaluate covariance among the independent variables themselves and to weigh the influence of each predictor variable on calcification intensity. Values for each independent variable were determined using the $\delta^{18}O$-derived calcification depths for each sample (described in section 4.3).

Simple linear regressions (SLR) indicate that *G. bulloides* area density correlates significantly with all three of the predictor variables ([CO_3^{2-}] $R^2 = 0.80$, temperature $R^2 = 0.70$, and [PO_4^{3-}] $R^2 = 0.54$); with the highest-correlation coefficients observed between area density and [CO_3^{2-}] and temperature (Table S1 in the supporting information). SLR between the independent variables themselves also indicate that significant correlations exist between the variables; temperature is positively correlated with [CO_3^{2-}], and [PO_4^{3-}] is negatively correlated with [CO_3^{2-}] and temperature (Figure S7 in the supporting information). Because the SBB is influenced by seasonal upwelling, it is not surprising that the predictor variables covary, thus complicating a straightforward SLR approach. During early spring and summer months upwelling results in low-temperature waters depleted in [CO_3^{2-}] and enriched in nutrients being brought to the surface, resulting in collinearity among these environmental variables (Table S2 in the supporting information). In fact, multiple linear regression (MLR) statistics were used to quantify further the redundancy between the collinear independent variables using a stepwise multiple regression. By using a variable that is unrelated to the dependent variable, in this case, mean shell area, the shared variance between two independent variables, can be estimated. Using this method, we estimate that temperature and [CO_3^{2-}] are 86% redundant, while [PO_4^{3-}] and [CO_3^{2-}] are 65% redundant in our data set (Table S3 in the supporting information).

Due to the strong collinearity that exists between the independent variables used in this study, a number of statistical tests were conducted in attempt to disentangle these relationships. The issue of collinearity can be resolved by replacing measured values with calculated residual values. This approach was used in a series of stepwise hierarchal regressions analyses to model the influence of each predictor variable (Table S4 in the supporting information). The results of the four models indicate that [PO_4^{3-}] is not an important predictor variable while temperature and [CO_3^{2-}] are excellent predictors of area density. Although the results of our tests consistently suggest that [CO_3^{2-}] is more significantly related to area density than temperature, the tight collinearity that exists between these two independent variables (86% shared variance) resulted in very similar outcomes of our statistical tests. The covarying nature of temperature and [CO_3^{2-}] during our study period makes it nearly impossible to confidently distinguish their respective influences using only statistical tests. This highlights the need for an alternative approach to decouple the respective roles of these variables on *G. bulloides* calcification intensity.

4.6. Decoupling Temperature and [CO_3^{2-}]

We chose to further evaluate the influence of temperature and [CO_3^{2-}] on *G. bulloides* calcification intensity using a down core sediment record. As a result of increasing atmospheric CO_2 during the last 100 years, surface water [CO_3^{2-}] has been declining as a result of ocean acidification [e.g., *Gruber et al.*, 2012], while temperature has been increasing as a result of the greenhouse effect [e.g., *Field et al.*, 2006]. Thus, long-term trends in temperature and [CO_3^{2-}] are effectively decoupled during the last century as opposed to being tightly positively correlated as in our sediment trap study period. We use sea surface temperature data from the SBB (1955 up to present; 34°24.2′N, 119°41.6′W), sea surface salinity data from the Scripps Pier (1916 up to

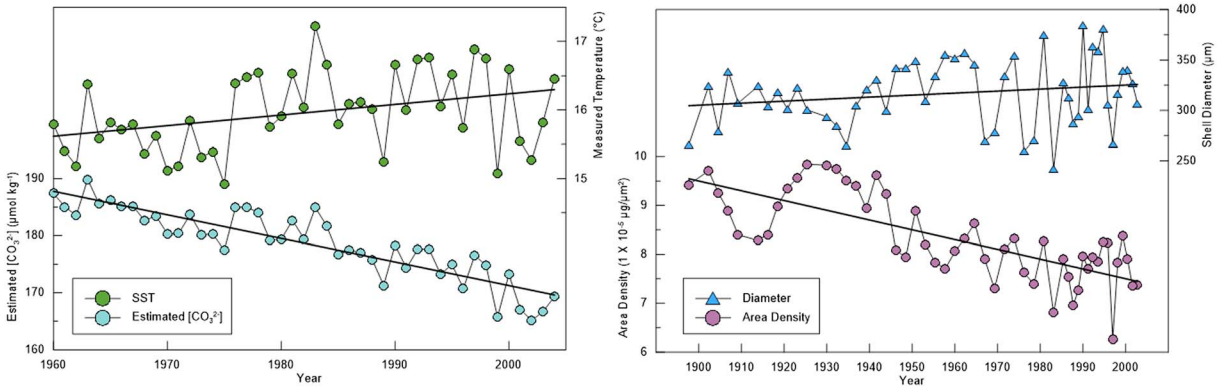

Figure 7. (left) Measured in situ sea surface temperature and estimates of surface [CO_3^{2-}] from the SBB (1955–2005). (right) Down core shell diameter and area density over the last century.

present; 32°52.0'N, 117°15.5'W), measured atmospheric CO_2 (1958 up to present; Mauna Loa), and assume a constant total alkalinity (2250 µmol kg^{-1}) to quantitatively estimate how [CO_3^{2-}] has changed over the last century in our study region (Text S4 in the supporting information). The inverse trends between temperature and [CO_3^{2-}] over this interval in our study region provide an opportunity to independently evaluate the influences of these variables on the calcification of *G. bulloides* (Figure 7).

Area density, shell diameter, and $\delta^{18}O$ measured on normal *G. bulloides* from the SBB box core are compared to the hydrographic time series of temperature and [CO_3^{2-}] (Figure 7). *Globigerina bulloides* $\delta^{18}O$ decreases over the sediment core and indicates roughly a 2°C warming, which is in good agreement with in situ measurements of temperature from the SBB (Figure S8 in the supporting information). Shell diameter increases while area density decreases over the 100 year down core data set. There is a significant and positive correlation between $\delta^{18}O$-derived temperature and mean shell diameter ($R^2 = 0.40$, $p < 0.001$). More importantly, there is an insignificant and negative correlation between temperature and area density ($R^2 = 0.11$, $p = 0.03$). The correlation between temperature and diameter supports previous observations that shell size is predominantly controlled by ambient temperature [e.g., *Schmidt et al*., 2004; *Lombard et al*., 2010]. The anticorrelation between temperature and area density indicates that correlations in our sediment trap observations are due simply to the collinearity between temperature and [CO_3^{2-}] during that study interval.

We use the linear regression between area density and [CO_3^{2-}] from our sediment trap observations (Figure 9) to estimate [CO_3^{2-}] from the down core area density values. A comparison of area density-[CO_3^{2-}] estimates to calculated surface [CO_3^{2-}] (1960–2005) indicates considerable agreement

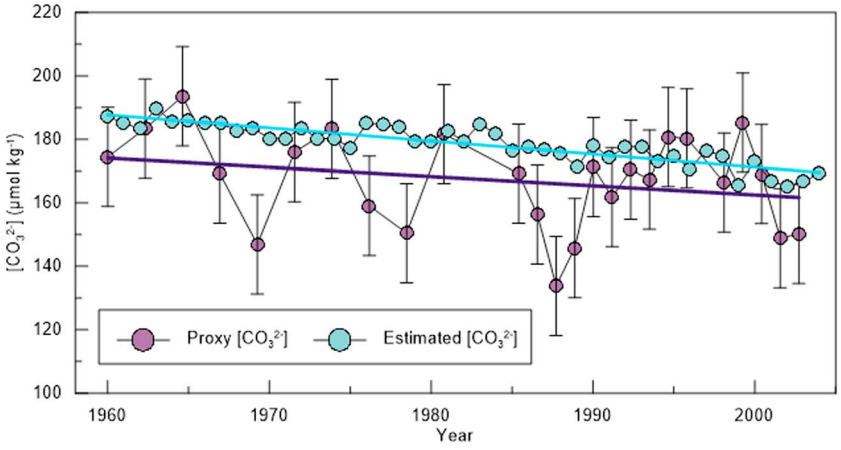

Figure 8. Comparison of calculated and area density-estimated [CO_3^{2-}]. Error bars on area density-[CO_3^{2-}] represent the standard error of the estimate from our sediment trap regression.

Table 1. Calibration Equations for the Normal and Encrusted *G. bulloides* Morphotypes Derived From our Sediment Trap Study

			Final Calibration Equations $Y = a + b(X)$					
Data	Y	X	a	b	R^2	p	Standard Error Estimate (Area Density)	Standard Error Estimate ($[CO_3^{2-}]$ μmol kg^{-1})
Normal ($n = 32$)	Area density	$[CO_3^{2-}]$	4.19E−5	1.92E−7	0.80	<0.001	3.00E−6	15.63
Encrusted ($n = 11$)	Area density	$[CO_3^{2-}]$	7.73E−5	1.58E−7	0.66	0.002	4.00E−6	25.40

between these records (Figure 8). Overall, both data sets indicate a similar long term declining trend although the $[CO_3^{2-}]$ estimated from area density measurements are generally lower, which is likely due to the fact that *G. bulloides* is not recording sea surface conditions. The increased variability observed in the proxy record is likely a product of calculated $[CO_3^{2-}]$ values not appropriately accounting for shifts in upwelling (Figure S9 in the supporting information). The proxy $[CO_3^{2-}]$ error represents the standard error of the estimate associated with our regression relationship and is typically within error of the calculated $[CO_3^{2-}]$.

4.7. Final Results and Comparison to Previous Work

While both temperature and $[PO_4^{3-}]$ could play some mediating role in calcification intensity, our hierarchical regression models and down core results indicate that these variables are secondary to $[CO_3^{2-}]$. In particular, the down core data indicate that calcification temperature affects shell size while $[CO_3^{2-}]$ is the dominant control on calcification intensity of *G. bulloides*. Based on our sediment trap observations, the relationships that exists between area density and $[CO_3^{2-}]$ for the normal and encrusted *G. bulloides* morphospecies are best described by linear relationships (Table 1 and Figure 9). The regression for encrusted *G. bulloides* is based on a limited number of observations and therefore has a low level of certainty. Due to the significant offset observed between *G. bulloides* morphospecies calcification intensity observed in this study, these calibration equations should be applied with caution to other *G. bulloides* morphospecies. While the normal

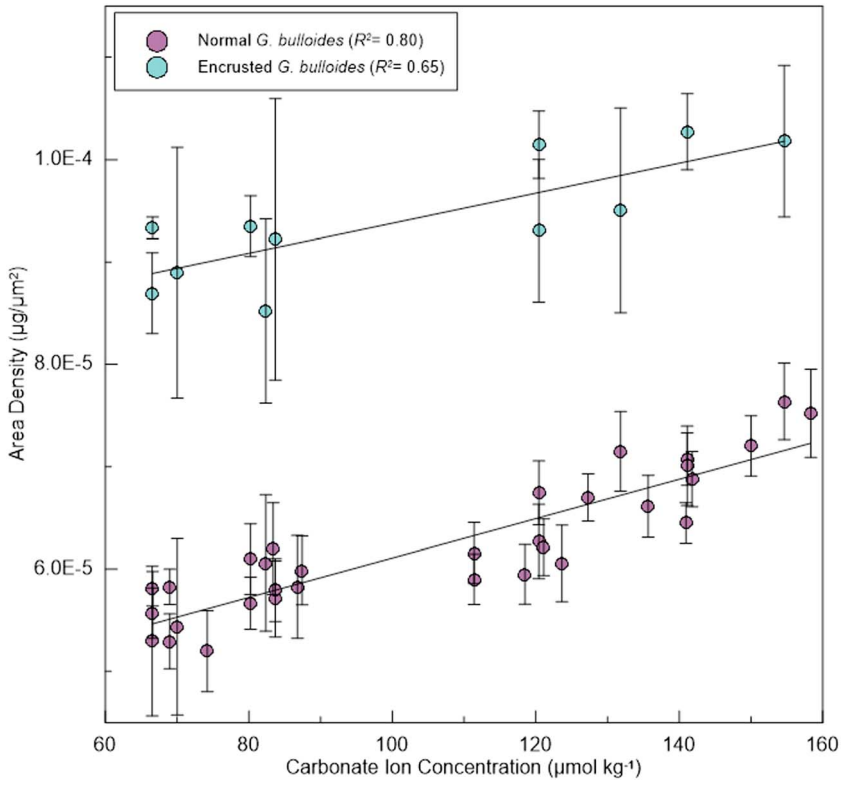

Figure 9. The linear relationship observed between normal and encrusted *G. bulloides* area density and $[CO_3^{2-}]$ from our sediment trap analyses. Error bars represent two standard errors ($SE = 2\sigma/\sqrt{n}$).

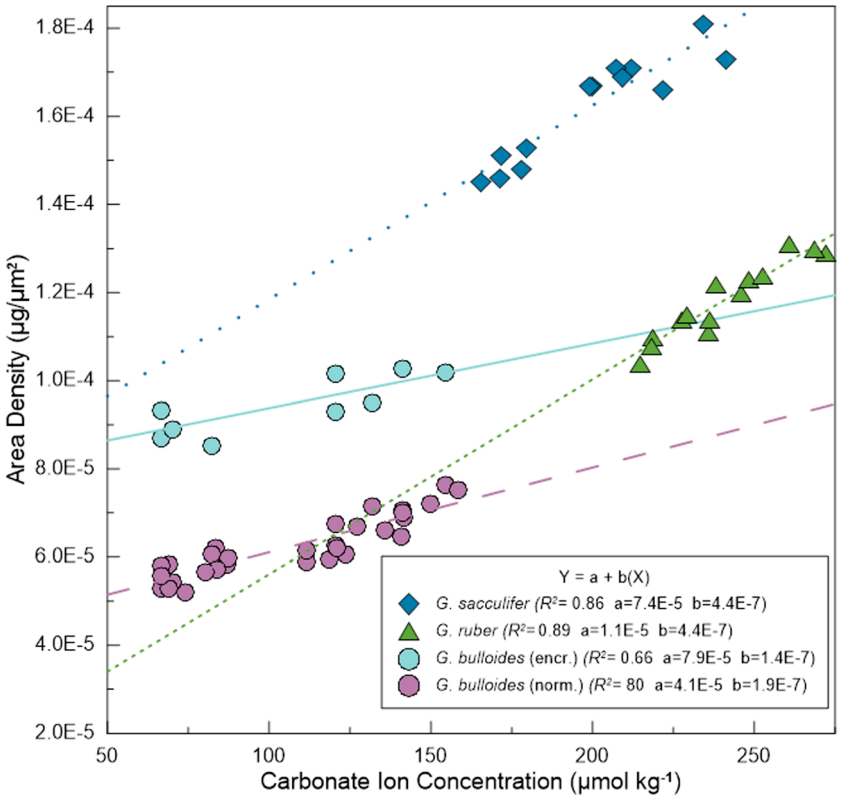

Figure 10. Comparison of area density calibrations for *G. bulloides* (normal and encrusted) (this study) and *G. ruber* and *G. sacculifer* [*Marshall et al*., 2013].

G. bulloides (genotype IIb) occurs over a range of sea surface temperatures (10–19°C) during both upwelling and nonupwelling periods it has not yet been observed in the Atlantic Ocean [*Darling et al*., 2003]. Therefore, our normal *G. bulloides* area density calibration may not be suitable for Atlantic morphotypes [*Stewart*, 2000; *Kucera and Darling,* 2002].

The results of our work agree well with several previous studies that have cited [CO_3^{2-}] as the dominant factor influencing *G. bulloides* calcification [*Barker and Elderfield,* 2002; *Gonzalez-Mora et al*., 2008; *Moy et al*., 2009]. The commonality among these previous studies is that they were all conducted using sediment core-top and down core records, making this the first sediment trap study to directly assess the relationship between in situ [CO_3^{2-}] and *G. bulloides* calcification. Another recent sediment trap study in the North Atlantic (Madeira Basin), where there are negligible changes in [CO_3^{2-}], evaluated the response of *G. bulloides* calcification intensity to temperature and productivity and also observed no significant response of SNSW to these variables [*Weinkauf et al*., 2016]. A laboratory culture that exposed *G. bulloides* to varying [CO_3^{2-}] found no conclusive influence on shell weight, but this is likely due to the fact that these weight measurements were not size normalized and that calcite added during culturing cannot be separated from precultured calcite [*Spero et al*., 1997].

While our results agree with much of the previous work on *G. bulloides* calcification, they also contrast with two studies that link *G. bulloides* calcification to nutrient concentration. Results from an Arabian Sea plankton tow (0–60 m) study suggested that the relationship observed between *G. bulloides* MBW and [CO_3^{2-}] ($R^2 = 0.4$) was not the product of a causal relationship and recommended investigating the influence of other environmental variables on calcification [*Beer et al*., 2010a]. In a follow up study, both SBW and MBW of *G. bulloides* (150–200 µm and 200–250 µm) from a North Atlantic plankton tow indicated a significant negative correlation with nutrient concentration leading the authors to suggest that increased nutrient content of seawater inhibits *G. bulloides* calcification [*Aldridge et al*., 2012]. As in the SBB, nutrient concentration ([PO_4^{3-} and [NO_3^-]) and [CO_3^{2-}] are closely linked in the North Atlantic ($R^2 = 0.72$ and 0.82, respectively) [*Aldridge et al*., 2012] making it difficult to determine the extent to which each variable affects calcification

intensity. It is also important to note that surface plankton tows (0–60 m) were used to collect the individuals used in both of these studies and therefore possibly contain a range of preadult ontogenic stages that would complicate shell weight analysis. Specifically, the authors indicate that some individuals from this study had not completed calcification of their final chamber [*Aldridge et al*., 2012]. Further, our work highlights the importance of pairing SNSW with ambient calcification conditions rather than simply surface conditions. This is particularly important for *G. bulloides* as its depth of calcification appears to be strongly related to the depth of the thermocline, which can vary significantly seasonally.

Several species-specific area density calibrations have been developed for tropical species using sediment trap samples from the Cariaco Basin [*Marshall et al*., 2013] providing a direct comparison to our area density results. Despite the differences in [CO_3^{2-}] ranges between studies, this comparison clearly indicates that strong interspecies differences exist and highlights the considerable offset even between *G. bulloides* morphospecies (Figure 10). The slopes of the symbiont-bearing species (*G. sacculifer* and *G. ruber*) are notably steeper than those recorded for symbiont-barren *G. bulloides* morphospecies. Some studies have suggested that the calcification in symbiont and nonsymbiont bearing species may respond differently to changes in carbonate chemistry. Species that harbor photosynthetic symbionts such as *G. ruber* and *G. sacculifer* have the ability to convert HCO_3^- to CO_3^{2-} via pH regulation thereby increasing ambient [CO_3^{2-}] and enhancing a microenvironment for calcification [*Jørgensen et al*., 1985; *Rink et al*., 1998]. For this reason *Aldridge et al.* [2012] suggested that due to a lack of symbionts, *G. bulloides* exhibit a larger change in shell weights [*Barker and Elderfield,* 2002] as compared to *G. ruber* [*de Moel et al*., 2009] since the Last Glacial Maximum. The interspecies comparison of area density calibrations suggests the opposite; symbiont-bearing species respond more dramatically to changes in [CO_3^{2-}] relative to the nonsymbiont bearing species. In order to fully assess the differences between the calcification intensity of symbiont-bearing and symbiont-barren foraminifera and [CO_3^{2-}], calibrations should be developed for additional foraminifera species.

5. Conclusions

Our results indicate that the calcification intensity of the planktonic foraminifera *G. bulloides* is significantly related to the ambient [CO_3^{2-}] making it an ideal species for reconstructions of surface ocean [CO_3^{2-}] from well-preserved sediments. The nondestructive nature of the area density method allows for [CO_3^{2-}] estimates to be directly coupled with geochemical measurements from a single sample population, which is an exciting prospect for developing multiproxy climate records. We also identify two cryptic morphospecies of *G. bulloides* that have been previously found in our study region using a combination of morphometric measurements. Due to the significant difference in calcification and offset in the stable isotopes observed between these morphospecies, we suggest using this morphometric technique as a means to identify cryptic species when generating paleoreconstructions using *G. bulloides*.

Acknowledgments

We would like to thank David Burdige from Old Dominion University for collecting the box core used in this study and Yongchen Wang for his assistance making seawater carbonate chemistry measurements. Reviews from Natalie Umling, Bärbel Hönisch, Manuel Weinkauf, and an anonymous reviewer greatly improved this manuscript. Thanks to Jay Pinckney for assistance and helpful review of the statistical analyses included in this study. We also acknowledge the Santa Barbara Coastal LTER and the California Coastal Ecosystem LTER for providing financial support to the Santa Barbara Basin sediment-trapping program. This research was funded in part by the National Science Foundation. The calibration and down core data sets created as a part of this study can be accessed in the supporting information. TA and DIC measurements made within the Santa Barbara Basin can be requested from Wei-Jun Cai (wcai@udel.edu) and temperature and nutrient data can be assessed from the Plumes and Blooms website (http://www.oceancolor.ucsb.edu/plumes_and_blooms/). Santa Barbara temperature measurements are collected by the City of Santa Barbara Harbor Patrol. Data are provided by the Shore Stations Program sponsored at Scripps Institution of Oceanography by California State Parks, Division of Boating and Waterways. Contact shorestation@ucsd.edu.

References

Aldridge, D., C. J. Beer, and D. A. Purdie (2012), Calcification in the planktonic foraminifera *Globigerina bulloides* linked to phosphate concentrations in surface waters of the North Atlantic Ocean, *Biogeosciences*, *9*(5), 1725–1739, doi:10.5194/bg-9-1725-2012.

Alin, S. R., R. A. Feely, A. G. Dickson, J. M. Hernandez-Ayon, L. W. Juranek, M. D. Ohman, and R. Goericke (2012), Robust empirical relationships for estimating the carbonate system in the southern California Current System and application to CalCOFI hydrographic cruise data (2005–2011), *J. Geophys. Res.*, *117*, C05033, doi:10.1029/2011JC007511.

Allen, K., B. Hönisch, S. Eggins, J. Yu, H. Spero, and H. Elderfield (2011), Controls on boron incorporation in cultured tests of planktic foraminifera *Orbulina universa*, *Earth Planet. Sci. Lett.*, *309*, 291–301.

Allen, K., B. Hönisch, S. Eggins, and Y. Rosenthal (2012), Environmental controls on B/Ca in calcite tests of the tropical planktic foraminifera species *Globigerinoides ruber* and *Globigerinoides sacculifer*, *Earth Planet. Sci. Lett.*, *351-352*, 270–280.

Barker, S., and H. Elderfield (2002), Foraminiferal calcification response to glacial-interglacial changes in atmospheric CO_2, *Science*, *297*, 833–836.

Bates, N. R., Y. M. Astor, M. J. Church, K. Currie, J. E. Dore, M. González-Dávila, L. Lorenzoni, F. Muller-Karger, J. Olafsson, and J. M. Santana-Casiano (2014), A time-series view of changing ocean chemistry due to ocean uptake of anthropogenic CO_2 and ocean acidification, *Oceanography*, *27*(1), 126–141.

Bé, A. W. H. (1977), An ecological, zoogeographic and taxonomic review of recent planktonic Foraminifera, in *Oceanic Micropalaeontology*, edited by A. T. S. Ramsay, pp. 1–100, Academic, London.

Bé, A. W. H., S. M. Harrison, and L. Lott (1973), *Orbulina universa* d'Orbigny in the Indian Ocean, *Mar. Micropaleontol.*, *19*(2), 150–192.

Beer, C. J., R. Schiebel, and P. A. Wilson (2010a), Testing planktic foraminiferal shell weight as a surface water [CO_3^{2-}] proxy using plankton net samples, *Geology*, *38*(2), 103–106.

Beer, C. J., R. Schiebel, and P. A. Wilson (2010b), Technical note: On methodologies for determining the size-normalised weight of planktic foraminifera, *Biogeosciences*, *7*(7), 2193–2198, doi:10.5194/bg-7-2193-2010.

Bemis, B. E., H. J. Spero, J. Bijma, and D. W. Lea (1998), Reevaluation of the oxygen isotopic composition of planktonic foraminifera: Experimental results and revised paleotemperature equations, *Paleoceanography*, *13*, 150–160, doi:10.1029/98PA00070.
Bemis, B. E., H. J. Spero, and R. C. Thunell (2002), Using species-specific paleotemperature equations with foraminifera: A case study in the Southern California Bight, *Mar. Micropaleontol.*, *46*, 405–430.
Berger, W. H. (1971), Sedimentation of planktonic foraminifera, *Mar. Geol.*, *11*, 325–358.
Bijma, J., H. J. Spero, and D. W. Lea (1999), Reassessing foraminiferal stable isotope geochemistry: Impact of the oceanic carbonate systems (experimental results), in *Use of Proxies in Paleoceanography: Examples From the South Atlantic*, edited by G. Fisher and G. Wefer, pp. 489–512, Springer, New York.
Bijma, J., B. Honisch, and R. E. Zeebe (2002), Impact of the ocean carbonate chemistry on living foraminiferal shell weight: Comment on "Carbonate ion concentration in glacial-age deep waters of the Caribbean Sea" by W. S. Broecker and E. Clark, *Geochem. Geophys. Geosyst.*, *3*(11), 1064, doi:10.1029/2002GC000388.
Broecker, W., and E. Clark (2001), A dramatic Atlantic dissolution event at the onset of the last glaciation, *Geochem. Geophys. Geosyst.*, *2*(11), 1065, doi:10.1029/2001GC000185.
Curry, W. B., and R. K. Matthews (1981), Equilibrium ^{18}O fractionation in small size fraction planktic foraminifera: Evidence from Recent Indian Ocean sediments, *Mar. Micropaleontol.*, *6*, 327–337.
Darling, K. F., and C. M. Wade (2008), The genetic diversity of planktic foraminifera and the global distrubtion of ribosomal RNA genotypes, *Mar. Micropaleontol.*, *67*, 216–238.
Darling, K. F., C. M. Wade, D. Kroon, A. J. Leigh Brown, and J. Bijma (1999), The diversity and distribution of modern planktonic foraminiferal small subunit ribosomal RNA genotypes and their potential as tracers of present and past ocean circulations, *Paleoceanography*, *14*, 3–12, doi:10.1029/1998PA900002.
Darling, K. F., C. M. Wade, I. A. Steward, D. Kroon, R. Dingle, and A. J. Leigh Brown (2000), Molecular evidence for genetic mixing of Arctic and Antarctic subpolar populations of planktonic foraminifers, *Nature*, *405*, 43–47.
Darling, K. F., M. Kucera,C. M. Wade, P. von Langen, and D. Pak (2003), Seasonal occurrence of genetic types of planktonic foraminiferal morphospecies in the Santa Barbara Channel, *Paleoceanography, 18*(2), 1032, doi:10.1029/2001PA000723.
de Moel, H., G. M. Ganssen, F. J. C. Peeters, S. J. A. Jung, D. Kroon, G. J. A. Brummer, and R. E. Zeebe (2009), Planktic foraminiferal shell thinning in the Arabian Sea due to anthropogenic ocean acidification?, *Biogeosciences*, *6*, 1917–1925.
de Villiers, S. (2004), Optimum growth conditions as opposed to calcite saturation as a control on the calcification rate and shell-weight of marine foraminifera, *Mar. Biol.*, *144*(1), 45–49, doi:10.1007/s00227-003-1183-8.
Dickson, A. G. (1990), Standard potential of the reaction: AgCl(s) + ½ H2(g) = Ag(s) + HCl(aq), and the standard acidity constant of the ion HSO4 in synthetic sea water from 273.15 to 318.15 K, *J. Chem. Thermodyn.*, *22*, 113–127.
Dickson, A. G., and F. J. Millero (1987), A comparison of the equilibrium constants for the dissociation of carbonic acid in seawater media, *Deep Sea Res.*, *34*, 1733–1743.
Dittert, N., and R. Henrich (2000), Carbonate dissolution in the South Atlantic Ocean: Evidence from ultrastructire breakdown in *Globigerina bulloides*, *Deep Sea Res., Part I*, *47*, 603–620.
Fairbanks, R. G., M. Sverdlove, R. Free, P. H. Wiebe, and A. W. H. Bé (1982), Vertical distribution and isotopic fractionation of living planktonic foraminifera from the Panama Basin, *Nature*, *298*, 841–844, doi:10.1038/298841a0.
Feely, R. A., C. L. Sabine, K. Lee, W. Berelson, J. Kleypas, V. J. Fabry, and F. J. Millero (2004), Impact of anthropogenic CO_2 on the $CaCO_3$ system in the oceans, *Science*, *305*, 362–366, doi:10.1126/science.1097329.
Field, D., D. Cayan, and F. Chavez (2006), Secular warming in the California Current and North Pacific, *CalCOFI Rep.*, *47*, 1–17.
Foster, G. L. (2008), Seawater pH, pCO_2 and $[CO_3^{2-}]$ variations in the Caribbean Sea over the last 130 kyr: A boron isotope and B/Ca study of planktic foraminifera, *Earth Planet. Sci. Lett.*, *271*, 254.
Friddell, J. E., R. C. Thunell, T. P. Guilderson, and M. Kashgarian (2003), Increased northeast Pacific climatic variability during the warm middle Holocene, *Geophys. Res. Lett., 30*(11), 1560, doi:10.1029/2002GL016834.
Ganssen, G., and M. Sarnthein (1983), Stable isotope composition of foraminifers: The surface and bottom water record of coastal upwelling, in *Coastal Upwelling: Its Sedimentary Record—Part A*, edited by J. Thiede and E. Suess, pp. 99–121, Plenum, New York.
Ganssen, G. M., F. J. C. Peeters, B. Metcalfe, P. Anand, S. J. A. Jung, D. Kroon, and G.-J. Brummer (2011), Quantifying sea surface temperature ranges of the Arabian Sea for the past 2000 years, *Clim. Past*, *7*, 1337–1349.
Gonzalez-Mora, B., F. J. Sierro, and J. A. Flores (2008), Controls of shell calcification in planktonic foraminifers, *Quat. Sci. Rev.*, *27*(9–10), 956–961, doi:10.1016/j.quascirev.2008.01.008.
Gruber, N., C. Hauri, Z. Lachkar, D. Loher, T. L. Frölicher, and G. Plattner (2012), Rapid progression of ocean acidification in the California current system, *Science*, *337*, 220–223.
Hecht, A. D. (1976), An ecologic model for test size variation in recent planktonic foraminifera: Applications to the fossil record, *J. Foraminiferal Res.*, *6*(4), 295–311, doi:10.2113/gsjfr.6.4.295.
Hemleben, C., M. Spintiler, and O. R. Anderson (1989), *Modern Planktonic Foraminifera*, 363 pp., Springer, New York.
Hendershott, M., and C. Winant (1996), Surface circulation in the Santa Barbara Channel, *Oceanography*, *9*, 114–121.
Hendy, I., and J. Kennett (1999), Latest quaternary North Pacific surface-water responses imply atmosphere-driven climate instability, *Geology*, *27*(4), 291–294.
Hendy, I. L., and J. P. Kennett (2000), Dansgaard-Oeschger cycles and the California Current System: Planktonic foraminiferal response to rapid climate change in Santa Barbara Basin, Ocean Drilling Program hole 893A, *Paleoceanography*, *15*, 30–42, doi:10.1029/1999PA000413.
Henehan, M., et al. (2013), Calibration of the boron isotope proxy in the planktonic foraminifera *Globigerinoides ruber* for use in paleo-CO_2 reconstruction, *Earth Planet. Sci. Lett.*, *364*, 111–122.
Hut, G. (1987), *Stable Isotope Reference Samples for Geochemical and Hydrological Investigations*, Int. At. Energy Agency, Vienna.
Jansen, H., R. E. Zeebe, and D. A. Wolf-Gladrow (2002), Modeling the dissolution of settling $CaCO_3$ in the ocean, *Global Biogeochem. Cycles*, *16*(2), 1027, doi:10.1029/2000GB001279.
Jørgensen, B. B., J. Erez, N. P. Revsbech, and Y. Cohen (1985), Symbiotic photosynthesis in a planktonic foraminiferan, *Globigerinoides sacculifer* (Brady), studied with microelectrodes, *Limnol. Oceanogr.*, *30*(6), 1253–1267.
Killingley, J. S., R. F. Johnson, and A. N. D. W. H. Berger (1981), Oxygen and carbon isotopes of individual shells of planktonic foraminifera from Ontong-Java Plateau, equatorial Pacific, *Palaeogeogr. Palaeoclimatol. Palaeoecol.*, *33*, 193–204.
Kincaid, E., R. Thunell, C. Lange, and A. Weinheimer (2000), Plankton fluxes in the Santa Barbara Basin: Response to seasonal and interannual changes, *Deep Sea Res.*, *47*, 1157–1176.
Kinsey, D. W., and P. J. Davies (1979), Effects of elevated nitrogen and phosphorous on coral reef growth, *Limnol. Oceanogr.*, *24*, 935–940.

Kroon, D., and G. Ganssen (1988), Northern Indian Ocean upwelling cells and the stable isotope composition of living planktic foraminifers, in *Planktonic Foraminifers as Tracers of Ocean-Climate History*, edited by G.-J. Brummer and D. Kroon, pp. 299–317, Free Univ. Press, Amsterdam.
Kucera, M., and K. F. Darling (2002), Genetic diversity among modern planktonic foraminifer species: Its effect on paleoceanographic reconstructions, *Philos. Trans. R. Soc. London, Ser. A*, *360*, 695–718.
Lee, K., T.-W. Kim, R. H. Byrne, and Y.-M. Liu (2010), The universal ratio of boron to chlorinity for the North Pacific and North Atlantic Oceans, *Geochim. Cosmochim. Acta*, *74*(6), 1801–1811.
Lewis, E., and D. W. R. Wallace (1998), Program developed for CO_2 system calculations, ORNL/CDIAC-105, Carbon dioxide Inf. Anal. Cent. Oak Ridge Nat. Lab., U.S. Dep. of Energy, Oak Ridge, Tenn.
Lin, Y.-P., and P. C. Singer (2006), Inhibition of calcite precipitation by orthophosphate: Speciation and thermodynamic considerations, *Geochim. Cosmochim. Acta*, *70*, 2530–2539.
Lombard, F., J. Erez, E. Michel, and L. Labeyrie (2009), Temperature effect on respiration and photosynthesis of the symbiont-bearing planktonic foraminifera *Globigerinoides ruber*, *Orubulina universa*, and *Globigerinella siphonifera*, *Limnol. Oceanogr.*, *54*(1), 210–218.
Lombard, F., R. E. da Rocha, J. Bijma, and J. P. Gattuso (2010), Effect of carbonate ion concentration and irradiance on calcification in planktonic foraminifera, *Biogeosciences*, *7*(1), 247–255, doi:10.5194/bg-7-247-2010.
Manno, C., N. Morata, and R. Bellerby (2012), Effect of ocean acidification and temperature increase on the planktonic foraminifer *Neogloboquadrina pachyderma* (sinistral), *Polar Biol.*, *35*, 1311–1319.
Marshall, B. J., R. Thunell, M. Hennehan, Y. Astor, and K. Wejnert (2013), Planktonic foraminiferal area density as a proxy for carbonate ion concentration: A calibration study using the Cariaco Basin ocean time series, *Paleoceanography*, *28*, 363–376, doi:10.1002/palo.20034.
Marshall, B. J., R. C. Thunell, H. J. Spero, M. J. Henehan, L. Lorenzoni, and Y. Astor (2015), Morphometric and stable isotopic differentiation of *Orbulina universa* morphotypes from the Cariaco Basin, Venezuela, *Mar. Micropaleontol.*, *120*, 46–64.
Mehrbach, C., C. H. Culberson, J. E. Hawley, and R. N. Pytkowicz (1973), Measurement of the apparent dissociation constants of carbonic acid in seawater at atmospheric pressure, *Limnol. Oceanogr.*, *18*, 897–907.
Mekik, F., and L. Raterink (2008), Effects of surface ocean conditions on deep-sea calcite dissolution proxies in the tropical Pacific, *Paleoceanography*, *23*, PA1216, doi:10.1029/2007PA001433.
Milliman, J. D., P. J. Troy, W. M. Balch, A. K. Adams, Y.-H. Li, and F. T. Mackenzie (1999), Biologically mediated dissolution of calcium carbonate above the chemical lysocline?, *Deep Sea Res., Part I*, *46*, 1653–1669.
Moore, W. S. (1984), Radium isotope measurements using germanium detectors, *Nucl. Instrum. Methods Phys. Res.*, *223*(2–3), 407–411.
Moy, A. D., W. R. Howard, S. G. Bray, and T. W. Trull (2009), Reduced calcification in modern Southern Ocean planktonic foraminifera, *Nat. Geosci.*, *2*, 276–280.
Paasche, E., and S. Brubank (1994), Enhanced calcification in the coccolithophorid *Emiliania huxleyi* (Haptophyceae) under phosphorus limitation, *Phycologia*, *22*, 324–330.
Pak, D. K., D. W. Lea, and J. P. Kennett (2004), Seasonal and interannual variation in Santa Barbara Basin water temperatures observed in sediment trap foraminiferal Mg/Ca, *Geochem. Geophys. Geosyst.*, *5*, Q12008, doi:10.1029/2004GC000760.
Pak, D. K., D. W. Lea, and J. P. Kennett (2012), Millennial scale changes in sea surface temperature and ocean circulation in the northeast Pacific, 10–60 kyr BP, *Paleoceanography*, *27*, PA1212, doi:10.1029/2011PA002238.
Peeters, F., E. Ivanova, S. Conan, G.-J. Brummer, G. Ganssen, S. Troelstra, and J. van Hinte (1999), A size analysis of planktic Foraminifera from the Arabian Sea, *Mar. Micropaleontol.*, *36*(1), 31–61.
Pierrot, D., E. Lewis, and D. W. R. Wallace (2006), MS Excel program developed for CO_2 system calculations, ORNL/CDIAC-105a, Carbon Dioxide Inf. Anal. Cent., Oak Ridge Natl. Lab., U.S. Dep. of Energy, Oak Ridge, Tenn.
Prell, W. L., and W. B. Curry (1981), Faunal and isotopic indices of monsoonal upwelling: Western Arabian Sea, *Oceanol. Acta*, *4*, 91–98.
Rae, J. W. B., G. L. Foster, D. N. Schmidt, and T. Elliott (2011), Boron isotopes and B/Ca in benthic foraminifera: Proxies for the deep ocean carbonate system, *Earth Planet. Sci. Lett.*, *302*, 403–413.
Reimers, C. E., M. Kastern, and R. E. Garrison (1990), The role of bacteria mats in phosphate mineralization with particular reference to the Monterey Formation, in *Phosphate Deposits of the World*, vol. 3, edited by W. C. Burnett and S. R. Riggs, pp. 300–311, Cambridge Univ. Press, Cambridge, U. K.
Rink, S., M. Kuhl, J. Bijma, and H. J. Spero (1998), Microsensor studies of photosynthesis and respiration in the symbiotic foraminifer *Orbulina universa*, *Mar. Biol.*, *131*, 583–595.
Sanyal, A., N. G. Hemming, W. S. Broecker, D. W. Lea, H. J. Spero, and G. N. Hanson (1996), Oceanic pH control on the boron isotopic composition of foraminifera: Evidence from culture experiments, *Paleoceanography*, *11*, 513–517, doi:10.1029/96PA01858.
Sautter, L. R., and R. C. Thunell (1991a), Planktonic foraminiferal response to upwelling and seasonal hydrographic conditions: Sediment trap results from San Pedro Basin, Southern California Bight, *J. Foraminiferal Res.*, *21*(4), 347–363.
Sautter, L. R., and R. C. Thunell (1991b), Seasonal variability in the $\delta^{18}O$ and $\delta^{13}C$ of planktonic foraminifera from an upwelling environment: Sediment trap results from the San Pedro Basin, Southern California Bight, *Paleoceanography*, *6*, 307–334, doi:10.1029/91PA00385.
Schiebel, R. (2002), Planktonic foraminiferal sedimentation and the marine calcite budget, *Global Biogeochem. Cycles, 16*(4), 1065, doi:10.1029/2001GB001459.
Schiffelbein, P., and S. Hills (1984), Direct assessment of stable isotope variability in planktonic foraminifera populations, *Palaeogeogr. Palaeoclimatol. Palaeoecol.*, *48*, 197–213.
Schmidt, D. N., S. Renaud, J. Bollmann, R. Schiebel, and H. R. Thierstein (2004), Size distribution of Holocene planktic foraminifer assemblages: Biogeography, ecology and adaptation, *Mar. Micropaleontol.*, *50*(3-4), 319–338, doi:10.1016/S0377-8398(03)00098-7.
Spero, H. J., J. Bijma, D. W. Lea, and B. E. Bemis (1997), Effect of seawater carbonate concentration on foraminiferal carbon and oxygen isotopes, *Nature*, *390*(6659), 497–500.
Stewart, I. A. (2000), The molecular evolution of planktonic foraminifera and its implications for the fossil record, PhD thesis, Univ. of Edinburgh, Edinburgh, U. K.
Takahashi, T., R. T. Williams, and D. L. Bos (1982), Carbonate chemistry, in *GEOSECS Pacific Expedition*, *Hydrographic Data 1973–1974*, vol. 3, edited by W. S. Broecker, D. S. Spencer, and H. Craig, pp. 77–83, Natl. Sci. Found., Washington, D. C.
Thiede, J. (1983), Skeletal plankton and nekton in upwelling water masses off northwestern South America and northwestern Africa, in *Coastal Upwelling: Its Sedimentary Record—Part A*, edited by J. Thiede and E. Suess, pp. 183–208, Plenum, New York.
Thunell, R. (1998), Particle fluxes in a coastal upwelling zone: Sediment trap results from Santa Barbara Basin, California, *Deep Sea Res.*, *45*, 1863–1884.
Thunell, R., R. S. Keir, and S. Honjo (1981), Calcite dissolution: An in situ study from the Panama Basin, *Science*, *212*(4495), 659–661.
Thunell, R., E. Tappa, and D. Anderson (1995), Sediment fluxes and varve formation in Santa Barbara Basin, offshore California, *Geology*, *23*, 1083–1086.

Thunell, R., C. Benitez-Nelson, R. Varela, Y. Astor, and F. Muller-Karger (2007), Particulate organic carbon fluxes along upwelling-dominated continental margins: Rates and mechanisms, *Global Biogeochem. Cycles*, *21*, GB1022, doi:10.1029/2006GB002793.

Thunell, R. C., E. Tappa, C. Pride, and E. Kincaid (1999), Sea-surface temperature anomalies associated with the 1997–1998 El Niño recorded in the oxygen isotope composition of planktonic foraminifera, *Geology*, *27*(9), 843–846.

Weinkauf, M. F. G., T. Moller, M. C. Koch, and M. Kučera (2013), Calcification intensity in planktonic foraminifera reflects ambient conditions irrespective of environmental stress, *Biogeosciences*, *10*(10), 6639–6655.

Weinkauf, M. F. G., J. G. Kunze, J. J. Waniek, and M. Kučera (2016), Seasonal variation in shell calcification of planktonic Foraminifera in the NE Atlantic reveals species-specific response to temperature, productivity, and optimum growth conditions, *Plos One*, *11*(2), e148363.

Weiss, R. F. (1974), Carbon dioxide in water and seawater: the solubility of a non-ideal gas, *Mar. Chem.*, *2*, 203-215.

Yu, J., H. Elderfield, and B. Honisch (2007), B/Ca in planktonic foraminifera as a proxy for surface seawater pH, *Paleoceanography*, *22*, PA2202, doi:10.1029/2006PA001347.